TEKSTİL VE MÜHENDİS

(Journal of Textiles and Engineer)

http://www.tekstilvemuhendis.org.tr

SMART TEXTILE pH SENSOR BASED ON CURCUMIN MICROCAPSULES

ZERDEÇAL MİKROKAPSÜL ESASLI AKILLI TEKSTİL pH SENSÖRÜ

Fabien SALAÜN

Univ. Lille, ENSAIT, ULR 2461 - GEMTEX - Génie et Matériaux Textiles, F-59000 Lille, France

Online Erişime Açıldığı Tarih (Available online):31 Aralık 2023 (31 December 2023)

Bu makaleye atıf yapmak için (To cite this article):

Fabien SALAÜN (2023): Smart Textile Ph Sensor Based On Curcumin Microcapsules, Tekstil ve Mühendis, 30: 132, 310- 317.

For online version of the article: https://doi.org/10.7216/teksmuh.1406050

Araştırma Makalesi / Research Article

SMART TEXTILE pH SENSOR BASED ON CURCUMIN MICROCAPSULES

Fabien SALAÜN

Univ. Lille, ENSAIT, ULR 2461 - GEMTEX - Génie et Matériaux Textiles, F-59000 Lille, France

Gönderilme Tarihi / Received: 01.08.2023
Kabul Tarihi / Accepted: 15.12.2023

ABSTRACT: In this study, pH-sensitive textile systems are developed for use in detecting alkaline media variations. The product is designed based on the surface functionalization of cotton fabric by semi-porous microcapsules containing curcumin. The capsules synthesized by interfacial polymerization from MDI and xylitol serve as micro-reactors where a modification of the chemical form of curcumin takes place, allowing observation of a change of color. This change of color is linked to the acidity constant of this molecule. The objective is also to correlate the visual observation to an evaluation of the color code via image capture by a smartphone of the textile structure and simplified processing of the image color. The analyses have shown that the product obtained is well-sensitive to pH variations and easy to use.

Keywords: Curcumin, microencapsulation, chemical grafting, smart textile, pH sensor

ZERDEÇAL MİKROKAPSÜL ESASLI AKILLI TEKSTİL pH SENSÖRÜ

ÖZ: Bu çalışmada, alkali ortam değişimlerinin tespitinde kullanılmak üzere pH'a duyarlı tekstil sistemleri geliştirilmiştir. Bu ürün ile pamuklu kumaşın yüzeyi zerdeçal içeren yarı gözenekli mikrokapsüller ile fonksiyonelleştirilmiştir. MDI ve ksilitolden ara yüzey polimerizasyonuyla sentezlenen kapsüller, zerdeçalın kimyasal formunun modifikasyonunun gerçekleştiği mikro reaktörler olarak hizmet ederek renk değişiminin gözlemlenmesine olanak tanımıştır. Bu renk değişimi, molekülün asitlik sabiti ile bağlantılıdır. Çalışmada tekstil yapısının bir akıllı telefon yardımıyla görüntülenmesi ve görüntü renginin basitleştirilmiş bir şekilde işlenmesiyle renk kodunun değerlendirilmesi de amaçlanmıştır. Analizler, elde edilen ürünün pH değişimlerine karşı oldukça duyarlı ve kullanımının kolay olduğunu göstermiştir.

Anahtar Kelimeler: Zerdeçal, mikrokapsülasyon, kimyasal aşılama, akıllı tekstil, pH sensörü

Sorumlu Yazarlar/Corresponding Author: *fabien.salaun@ensait.fr*
DOI: *https://doi.org/10.7216/teksmuh.1406050* *www.tekstilvemuhendis.org.tr*

This study was presented at "8th International Technical Textile Congress (ITTC2022)", October 13-14, 2022, Online Congress. Peer review procedure of the Journal was also carried out for the selected papers before publication.

1. INTRODUCTION

pH tests are commonly used in chemistry laboratories to measure the acidity or alkalinity levels of solutions. There are various technologies for measuring pH values, but the most accurate pH measurements can be obtained with a pH meter. For these reasons, many researchers have begun to look for new methods to determine pH values. With the help of computer technology, many processes can be simplified and performed in a shorter time. Today, digital image processing and analysis methods have gained popularity in these applications [1, 2].

The most common and convenient way to use pH paper is to measure acidity, basicity and pH concentration by changing the color. A pH paper is a paper made by infiltrating an indicator into a filter paper with a color change occurring as a result of the reaction depending on the hydrogen ion concentration of the solution. The pH of the solution can be determined by observing the color change and comparing it to the standard discoloration table. This method has the following advantages: simple and fast measurement Colorimetric indicators such as pH sensitive dyes provide visual information. The pH value is an important parameter in many circumstances and therefore a halochromic textile could be used for various applications [3]. In this context, the textile structure can also be used to detect the pH of an environment [4].

Curcumin (1,7-bis(4-hydroxy-3-methoxyphenyl)-1,6-heptadiene-3,5-dione) is a bioactive component and a low molecular weight polyphenol of turmeric (*Curcuma longa L.)* which is widely used as a food colorant [5]. Curcumin has a yellow color, and the chemical structure presents two o-methoxy phenols attached symmetrically through α, β-unsaturated β-diketone linker, which also induces keto-enol tautomerism [6]. This compound is practically insoluble in water at acidic and neutral pH, and this stability is attributed to its conjugated diene structure. Furthermore, curcumin has three ionizable protons, one from the enolic proton and the two last from the two phenolic OH groups. The pKa values for dissociating the three acid protons have been estimated from 7.7 to 8.5, 8.5 to 10.4, and 9.5 to 10.7, respectively [7]. Thus, when the pH increases to neutral-basic conditions, a proton is removed from the enolic form and afterward from the phenolic group leading to the destabilization of the structure. Even if the solubility can be enhanced under alkaline conditions resulting in a color change of the chromophore groups to deep red, the pH modification caries to the instability and the destruction of this structure [8].

This paper studies the conventional finishing method to as possible approaches to obtain textile pH-sensors. Since curcumin can interact with the environment, it is necessary to protect it with a semi-porous polymeric membrane allowing the diffusion of the liquid into the core of the capsule to modify its chemical form, while ensuring the reversibility of the effect [9]. In addition, the chemical grafting method of the microcapsules was preferred to ensure the permeation of the membrane. The objective of this study is to investigate the influence of the rate of microcapsules required for pH detection, and to couple the visual measurement with simple image processing from capturing the functionalized media with a smartphone to edit the color code, as a simple alternative approach to determine pH values of different, was investigated.

2. MATERIAL AND METHOD

2.1 Reagents and Materials

1,7-Bis(4-hydroxy-3-methoxyphenyl)-1,6-heptadiene-3,5-dione (curcumin) was purchased from Aldrich (France) and used as core material. Diphenyl methylene diisocyanate (MDI) (Suprasec 2030, Hüntsman ICI), and xylitol (Roquette Frères, content >99%) ($C_5H_{12}O_5$), a polyhydric alcohol, were employed as shell-forming monomers for the interfacial polycondensation. Ethyl acetate (EtAc) (Fluka, France) and acetone (Merville, France) were used as solvents. Nonionic surfactant, Tween® 20 (Polyethylene glycol sorbitan monolaurate) was purchased from Aldrich and used as emulsifier. Sodium Dodecyl Sulfate (SDS) purchased from Aldrich (France) was used as surfactant. A 100% cotton twill fabric (TDV Industries, France) (296 g/m^2, air permeabilty 156 L/m^2/s, thickness 0.67 mm) was used as textile substrate.

2.2 Preparation of Curcumin Microcapsules

Curcumin microparticles were prepared by emulsion–diffusion technique, which is divided in four steps, i.e. mutual saturation, emulsification, diffusion and purification [10]. First, continuous (distilled water) and dispersed (ethyl acetate, EtAc) phases (2:1 v/v) were mutually saturated for 24 h to ensure thermodynamical equilibrium. The obtained solutions, aqueous and organic phases, contain 8.7% w/v of EtAc and 3% of water, respectively. Second, for the emulsification step, 0.5 g of curcumin and 2.9 g of MDI were dissolved in 30 ml of a binary mixture of acetone/ethyl acetate (1/2 v/v) saturated with water, and then this phase was emulsified with 60 ml of the aqueous phase containing 1.5 wt.% of Tween 20 at 4 °C, with the use of a high-speed homogenizer (Ultra-Turrax® T25 basic, Germany) at 6500 rpm during 50 min. After 25 min, when the expected droplet size of the emulsion was reached, the polymerization reaction was carried out by drop-wise addition of 10 ml of aqueous solution containing xylitol. The xylitol concentration was adjusted to obtain an NCO/OH mole ratio about 0.28, 0.138, 0.092, 0.069 and 0.0555. Third, to induce the formation of polymeric shell, the solution was transferred into a double walled four-necked vessel, the microparticles were maintained in suspension under a stirring speed of 500 rpm for 3 h. A large quantity of distilled water was subsequently added to the microemulsion inducing the diffusion of EtAc from the inner to the outer phase for the microsuspension. A volume equal to twice the volume of the emulsion was used for dilution. Finally, the resultant microparticles were recovered by filtration and washed twice with water, and then dried at 50 °C overnight, before being redispersed in water for further uses.

2.3 Preparation of Textile Based Curcumin Microparticles

In order to obtain the textile-based curcumin microparticles, microcapsules were applied to the surface of the fabric by bath exhaustion with a liquor ratio about 1:20, during one hour at 70°C before being dried in an oven at 130°C for 3 minutes. The solutions were prepared with different concentration of the microencapsulated curcumin, 60 g/L of Mikracat B and 10g/L of Mikrafix (obtained from Devan Chemicals, Belgium).

2.4 Characterization

2.4.1 Infrared spectra analyses

The chemical structure of the samples was analysed by infrared spectra in an absorbance mode, and recorded using Nicolet Nexus, connected to a PC, in which the number of scans was 256 and the resolution was 0.5 cm^{-1}. Samples were ground and mixed with KBr to make pellets. To put an interpretation on a more quantitative basis, we performed the de-convolution of the spectra using peakfit 4.0 software (Jandel, San Rafael, CA) in the 1575 - 1800 cm^{-1} region into Gaussian peaks. These wavenumbers were used as initial parameters for curve fitting with Gaussian component peaks. Position, bandwidths, and amplitudes of the peaks were varied until: (i) the resulting bands shifted by no more than 4 cm^{-1} from the initial parameters, (ii) all the peaks had reasonable half-widths (< 20-25 cm^{-1}), and (iii) good agreement between the calculated sum of all components and the experimental spectra was achieved ($r^2 > 0.99$). The results of four independent experiments were averaged.

2.4.2 Morphology of the particles

The microscopic aspects of the particles were observed by scanning electron microscopy (SEM) (Philips XL30 ESEM/EDAX – SAPPHIRE).

2.4.3 Thermal stability of the particles

The thermogravimetric analysis (TGA) was carried out using a TA Instrument TGA2950 apparatus under an inert atmosphere at a 50 ml/min purge rate. The heating rate of 10°C/min was used from 25 to 700 °C. For each experiment, approximately a 10.0 mg sample was used in the TGA test. TGA experiments were used to evaluate the thermal stability of the microcapsules shell, and they can also provide indirect information on shell structure and encapsulation yield.

2.4.4 pH Response of fabric sample

Functionalized textile fabrics were cut into squares (5 cm × 5 cm) and introduced into individual buffered solutions (20 mL, pH = 4, 5, 6, 7, 8, 9, 10, and 11) for 5 minutes, then removed with tweezers. The color changes of the textile-based pH sensors were captured and extracted using a spectrophotometer, Datacolor International SF 600 plus, interfaced with a personal computer. 10 detections were performed for each sample. A photographic image was captured using a smartphone camera at a distance of 10 cm from a designated angle. Because the color from a sensor is influenced by the angle owing to the nature of diffraction, the initial angle was fixed at 90°. Image treatment was realized to extracted in a simple way the values of Red, Blue and Green. The data obtained from these two ways were transformed to Y-greyscale values for comparison (greyscale=0.299*R + 0.587*G + 0.114 *B) [2].

3. RESULTS AND DISCUSSION

3.1 Formation and structure of the microparticles

Curcuminoids are readily soluble in polar organic solvents, but are sparingly soluble in water or hydrocarbons. Curcumin's 1,3-diketone group has keto-enol tautomerism, and thus exists in the tautomeric keto and enol forms. The keto form predominates in curcumin crystals or in acidic and neutral solutions, while the keto-enol form is exclusively present under alkaline conditions. Under acidic and neutral conditions, curcumin was relatively stable, with no change in color. Under alkaline conditions, the color changes from yellow to orange-brown. At pH 2-7, curcumin was stable and yellow in color, while at pH 8-13, it turned orange-brown. Consequently, as water solubility increases under alkaline conditions, this compound must be protected before use.

Curcumin microencapsulation was achieved by an emulsion solvent diffusion process, in which shell formation was promoted by the interfacial polycondensation of diisocyanate and xylitol (Figure 1). The process used was based on several consecutive steps, namely (i) the formation of a stable emulsion governing droplet size, (ii) a dilution step to induce ethyl acetate diffusion from the inner core of the droplet to the continuous governed by thermodynamic equilibrium, (iii) the interfacial reaction of the two monomers to promote polymeric shell formation. Diffusion of ethyl acetate changes the solvency of the reaction medium, of a solid shell entrapping curcumin.

The choice of solvents to form curcumin-containing microparticles was based on the physicochemical characteristics of curcumin and the polymeric shell to ensure emulsion establishment, followed by precipitation/formation of the polymeric shell at the interface. Shell formation during polycondensation requires precipitation of the oligomers initially formed to cover the droplets by modifying the solvency of the medium [11]. As the growth of this shell is achieved by the diffusion of one of the monomers through it, the formulation of the dispersed phase plays an important role. Based on the determination of the solubility parameters of curcumin (δ_d=17.4, δ_p=6.0 and δ_h=10.9 $MPa^{½}$) [12], acetone (δ_d=15.5, δ_p=10. 4 and δ_h=6.9 $MPa^{½}$) and ethyl acetate (δ_d=15.8, δ_p=5.3 and δ_h=7.2 $MPa^{½}$) were chosen as suitable solvents, and MDI as the fat-soluble monomer. Acetone is more polar than ethyl acetate, and the interactions of these solvents with water can be considered similar.

Dropwise, the addition of xylitol leads to the formation of insoluble oligomers in the droplets, which diffuse to the organic side of the interface to form a primary shell around the droplets. Membrane growth is based on further cross-linking reactions by monomer diffusion. Nevertheless, shell thickness increases slowly due to the restricted diffusion of starting monomers, inducing layer morphology and roughness changes. Capsule porosity increases with polymer precipitation at the interface and diffusion of solvent molecules through the wall. Solid membrane formation is linked to precipitation of the polymers formed due to non-solubility in the selected solvent media (polyurethane (δ_d=20.5, δ_p=6.4 and δ_h=13.0 $MPa^{½}$)).

The chemical reactions during membrane formation are illustrated in Figure 2. MDI monomers are slowly hydrolyzed on the organic side of the interface to form an unstable amino acid group, which dissociates into an amine end group and carbon dioxide. This reaction is initiated by the diffusion of water molecules through the polymer shell network. The formation and release of CO_2 contribute to an increase in particle porosity. In the second reaction, the amine end group reacts with the isocyanate end group to form a urea bond. In the third reaction, the diisocyanate or isocyanate end groups react with the hydroxyl groups of xylitol to form a urethane bond. Other secondary reactions are likely to occur during this step, forming an allophanate or biuret bridging the macromolecular chains.

An example of the FTIR absorption spectrum of the microcapsules is presented in Figure 3 (a), and the absence of a typical stretching absorption band at 2270 cm^{-1}, and the presence of the C O vibration between 1770 and 1600 cm^{-1} reveal that −NCO groups have reacted completely with the -OH group of xylitol. The absorption peaks corresponding to poly(urea-urethane) shell can be observed at around 3300 cm^{-1} (-OH and -NH stretching vibration), between 2920 and 2870 cm^{-1} for the C–H asymmetrical and symmetrical stretchings due to the methyl and methylene groups. C-O-C stretching at 1110 cm^{-1} and =C-H bending at 820 cm^{-1} are also present. N-H bending and C-N stretching at 1540 and 1236 cm^{-1} are also observed. The 1600, 1410, and 820 cm^{-1} peaks are assigned to the C=C stretching, C-C stretching, and C-H bending in aromatic groups, respectively. Since curcumin has many chemical similarities with the polymeric shell, confirmation of its entrapment can be confirmed by the presence of two thin shoulders at 1630 and 1280 cm^{-1}, assigned to the enol carbonyl stretching vibration and the C-O stretching, respectively. The C-O stretching is also present at 1160 cm^{-1} and 1031 cm^{-1}.

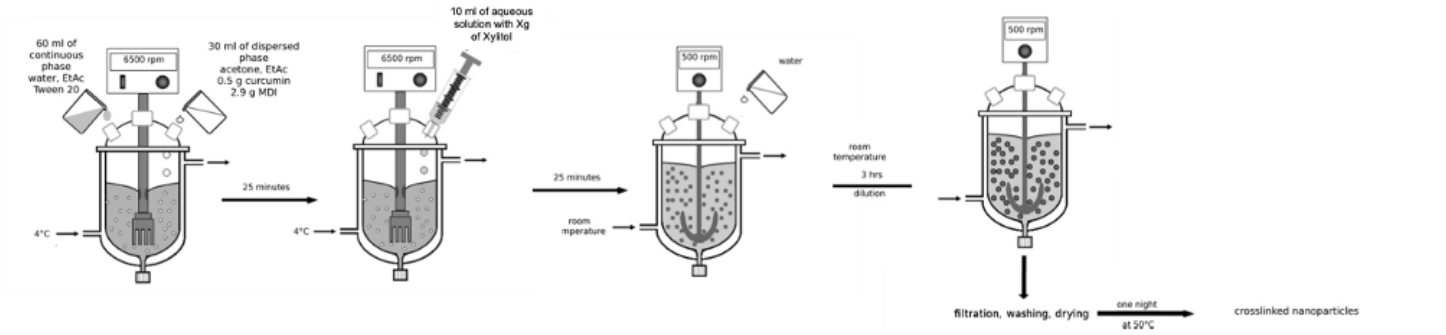

Figure 1. Schematic representation of the various stages of the microencapsulation process by the emulsion solvent diffusion method

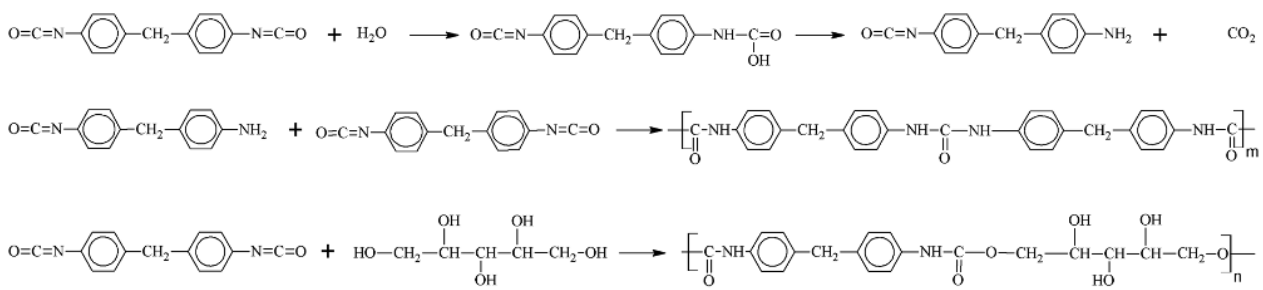

Figure 2. Chemical reactions leading to the formation of the microcapsule shell

3.2 Influence of the NCO/OH ratio on the structure of the microparticles

During shell formation, xylitol diffuses into the dispersed phase to react with MDI. Both the di-isocyanate and the amino oligomer formed are fat-soluble, which affects the course of polycondensation due to specific changes in phase composition. Formation of the swelling primary shell facilitates diffusion of xylitol and water molecules at the interface. It favors urea and urethane bonding, illustrated by the presence in the carbonyl region of a relatively sharp peak with a maximum at 1640 cm^{-1} and a thin shoulder at 1730 cm^{-1}, corresponding to C=O stretching of the free and bonded urea and urethane groups, respectively.

The formation of tinier particles during emulsification coupled with the diffusion of ethyl acetate leads to an increase in the surface area of the dispersed phase, favoriting the hydrolysis of the isocyanate group at the interface and thus the formation of urea bonds to the detriment of urethane bonds. The formation of these oligomers at the interface contributes to an increase in interface viscosity, which delays the diffusion of xylitol molecules through the shell, and therefore the formation of urethane bonds decreases as NCO/OH ratio (Figure 3).

The microencapsulation process and the NCO/OH ratio influence the particle size and their morphology (Figure 4). A high NCO/OH ratio leads to the formation of nanoparticles due to the spontaneous emulsion, allowing them to maintain the spherical shape during the first step of the polymerization course. The excess of xylitol promotes aggregation of the tiny particles, which collapse together to form irregular, rough microparticles. A slight decrease of xylitol limits the aggregation. The increase of xylitol induces changes in the formed particles' shape. The formation of more hydrophilic oligomers increases in the particle-to-particle interaction, which leads to the formation of aggregated submicronic particles to form irregular microparticles from 10 to 50 µm due to the macromolecular chain entanglements during the various steps of the process. Only at low ratios are spherical particles obtained. They have a rough surface, but closer examination revealed that the particles with broken membranes were hollow. This is due to the rapid polycondensation between the diisocyanate monomers and the small number of hydroxide functions, coupled with the diffusion of organic solvents in the aqueous medium.

The effect of the NCO/OH ratio on the thermal stability of the microparticles was also investigated. The TG curves of all samples have similar shapes. Degradation of the polyurea-urethane shell occurs in two consecutive stages, i.e. (i) from 200 to 340°C, linked to depolymerization of polyurethane units and oligomers leading to the formation of units cross-linked with urea groups; and (ii) from 340 to 700°C, there is initially recombination of urea oligomers up to 440°C and their degradation in a subsequent stage. The temperature corresponding to a 5% weight loss is the initial sample degradation temperature. The weight loss during the two degradation stages and the temperature at which degradation begins are correlated with the quantities of urethane and urea in the polymeric shell. Thus, the thermal stability of microparticles decreases with increasing urethane groups.

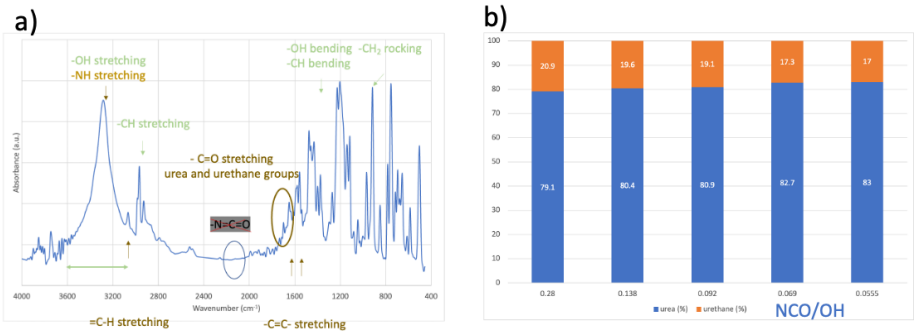

Figure 3. FTIR spectrum of curcumin microcapsules (NCO/OH=0.069) (a), and quantitative analysis of the urea–urethane region of FTIR spectra by peak deconvolution (b)

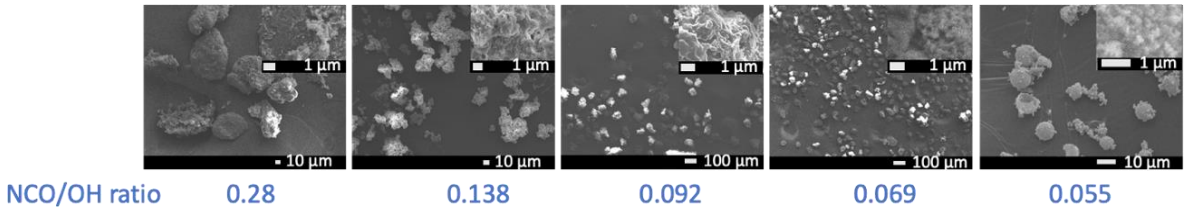

Figure 4. Influence of the NCO/OH ratio on the particles size and morphology.

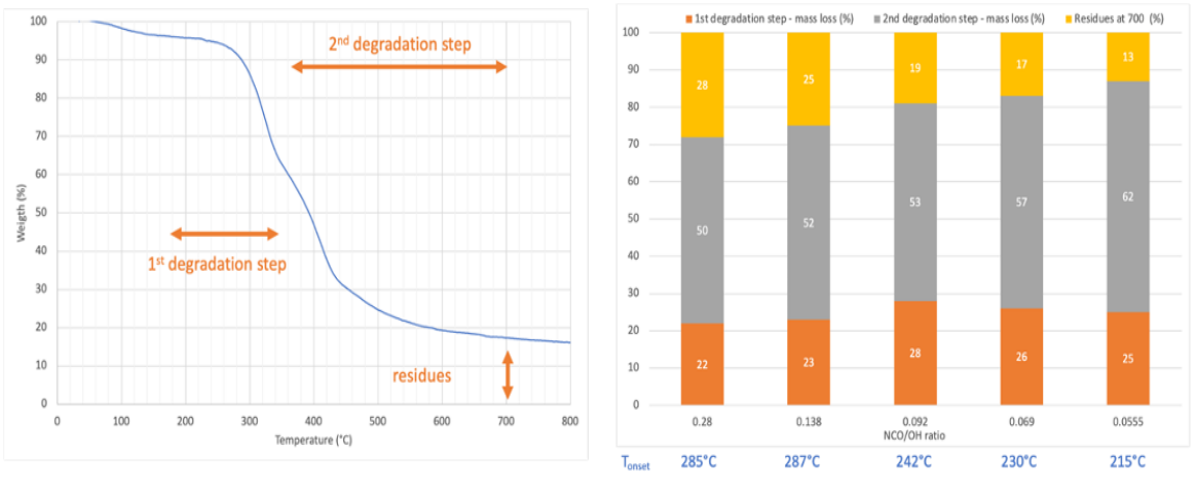

Figure 5. TG curve of microcapsule sample with an NCO/OH ratio of about 0.092 (left), and thermal stability data for different formulations (right).

The NCO/OH ratio when formulating the microparticle membrane influences the chemical structure of the membrane, with a modification of the urea and urethane functions. The number of hydroxyl functions modifies the polymerization kinetics, leading to different morphologies and hollow particles in the least favourable case. The thermal stability of the microparticles means they can be functionalized on textile substrates. Based on these results, an NCO/OH ratio of 0.092 was chosen for the rest of the study.

3.3 pH sensitive textile fabrics

3.3.1 Characteristics of pH sensor fabric at different pH values

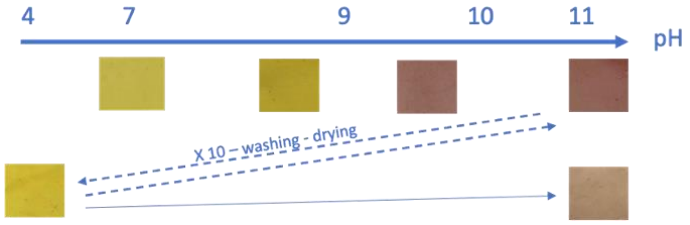

Figure 6. Color changes of test zones for the first test, and after 10 repetitions of pH tests and wash/dry cycles.

The pH dependence of the fabric-based microencapsulated curcumin was investigated by changing the pH of the solution from 4 to 11. Due to the porosity of the particle shell, the microcapsules act as a micro-reactor, allowing the diffusion of the aqueous solution in the inner core of the particles to react with curcumin molecules. At pH between 4 and 7, curcumin acts as a H-atom donor due to its keto form. From pH 8, curcumin acts as an electron donor since its enolate form predominates. Thus, a color change was observed from yellow to darker yellow until red at pH 9 and brown at pH 10 (Figure 6). All these color changes are also related to the pKa values: pKa_1 = 7.7-8.5, pKa_2 = 8.5-10.4, and pKa_3 = 9.5-10.7. After 10 repetitions of pH tests (from 4 to 11) and wash/dry cycles, the samples have the same initial color at low pH and a slight change at higher pH. The slight divergence underlines the stability of the pH-sensitive fabric's color change, with little degradation probably due to a hydrolysis reaction.

3.3.2 Influence of the amount of microcapsules on pH sensor fabric at pH = 7

The influence of the content of deposited microcapsules onto the textile fabric was studied to determine the most suitable amount for pH detection. The color of the samples at neutral pH (7.0) was used as a set point to establish the parameters for total variation in the fabric's color. The measured values of ⊗E do not allow us to distinguish between all the treated samples subjected to a neutral environment. All the calculated values range between 28 and 35 without being correlated to the microcapsule content. The samples became drastically darker (values of CIE L* are lower), less green (value of CIE a* increased), and no slight change was observed for the yellow since the values of CIE b* were positive and in the same range. The content of microparticles slightly influences the color of the textile support; the more microparticles there are, the more yellow predominates, and this in a uniform way on the surface of the samples at neutral pH. Figure 7 shows the RGB ratio according to the microcapsule concentration. The ratio of R is relatively high and reaches 40% from 3 wt.%, and the ratios of G and B do not vary much. Nevertheless, it was observed that the standard deviation decreased when the microcapsule content increased due to a better homogeneity of the finishing treatment. Thus, considering the reproducibility of the color change and the color homogeneity, surface treatment required 4 wt.% of microcapsules.

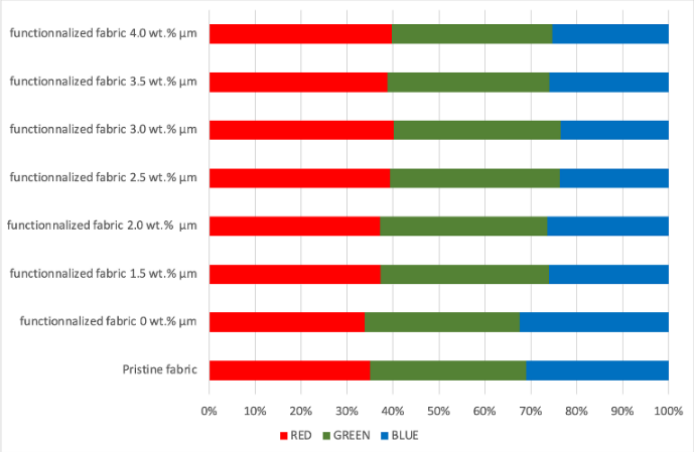

Figure 7. Influence of the amount of microcapsules at pH=7 on the RED, Blue and Green color ratio in the RGB space.

3.3.3 Characteristics of pH sensor fabric at different pH values

The pH-sensitive color change of the textile samples with 4 wt.% of microcapsules was also analytically assessed by analyzing the ⊗E values of the Datacolor spectrophotometer. The response of treated fabric to different pH solutions was examined for a functionalized fabric without microcapsules (i.e., control sample). The ⊗E values vary from 25 to 37, but only the L* value is correlated to the pH (R^2=0.88). The ratio of RGB was used to observe the color change. Until pH 6, no modification was observed; when the pH of the solution reached the pKa_1 of the curcumin, the ratio of B was increased, and the ratio of G was decreased. The ratio of R decreased only for pH close to the pKa_2 of curcumin, and the ratio of B was higher for pH in the range of pKa_3. Thus, it confirms the possibility of using the ratio of RGB to monitor color change versus the pH.

The changes in pH can be displayed visually in the numerical pH values with grey values data. This has the advantages of understanding the information intuitively and accessing it in a user-friendly way. Therefore, data will be readily understood, and trends will be identified easily (Figure 9). Through this method, a regression equation with a similar tendency to the original data was obtained from the two measurement ways, and the most appropriate formula was detected by comparing values of the coefficient of determination (R^2). The results show that both methods are correlated, and the data can be divided into three main ranges, i.e., (i) pH 4 to 6, (ii) pH 6 to 9, and (iii) pH higher than 9. Each inflection point corresponds to the pKa range.

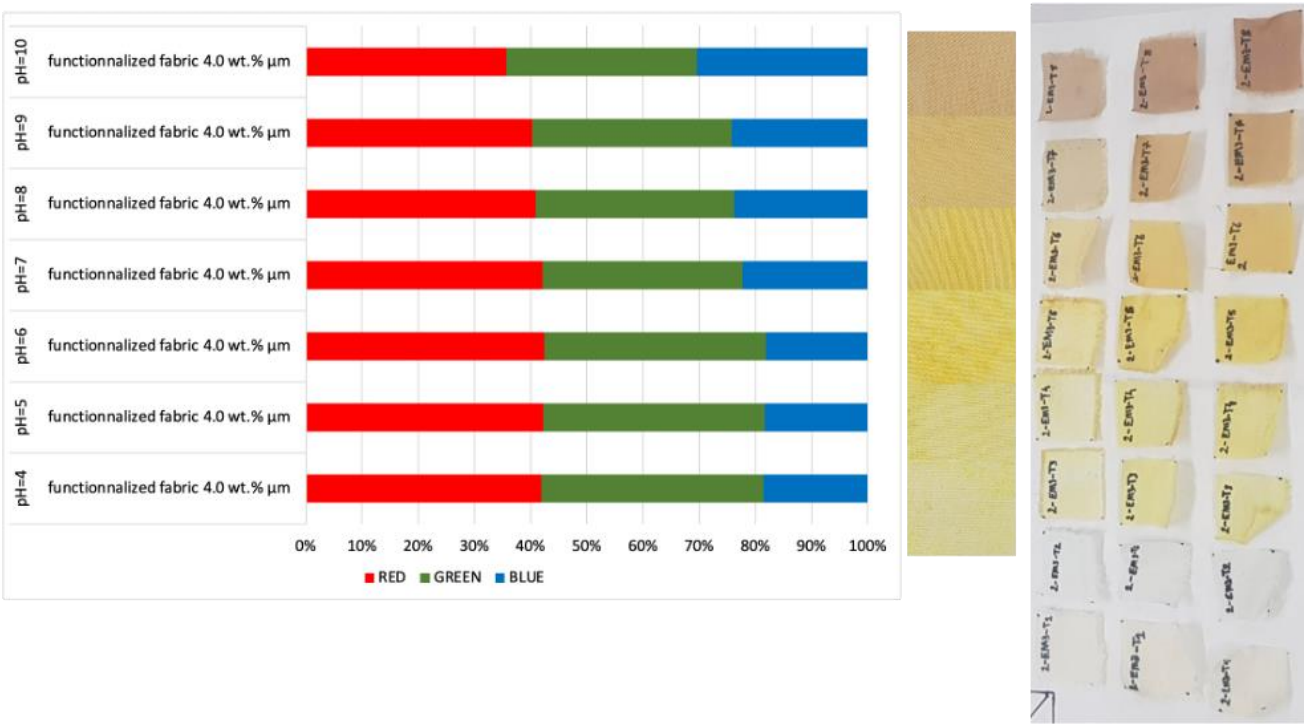

Figure 8. Influence of the pH on the color change of the fabric in the RBG color space (left), and images of the various samples (right).

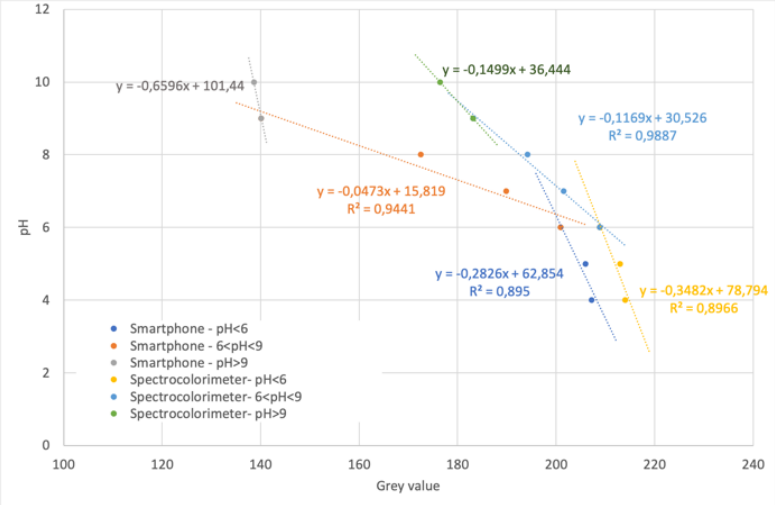

Figure 9. Relation between the grey value determined from the Red, Green and Blue values (smartphone and spectrocolorimeter) and pH.

4. CONCLUSION

This study suggests a new possibility of estimating pH by analyzing the color of pH-sensitive textiles, which is not a subjective method of visually assessing the degree of pH but quantitative data based on determining the color code of textile photographs. Curcumin was microencapsulated in a semi-porous polyurethane membrane. The influence of formulation parameters was used to provide information on the synthesis mechanism and to optimize the proportions of the two monomers. The capsules were then chemically grafted onto a textile substrate. Optimization of the rate of microcapsule deposition was based on the colorimetric response of the substrates, as well as their sensitivity to pH. The results showed that the textile support had become sensitive to pH and that it was possible to determine the pH of solutions using this material. The pH sensor developed has the advantage of being environmentally friendly thanks to using curcumin and textile microcapsules for sensor manufacture, requiring only a minimum of reagents and samples and not sophisticated instrumentation. What is more, it can be used up to 10 times. Evaluation of the results shows that the products have sufficient activity and sensitivity to detect the pH of the surrounding liquid medium. Exploiting the photographic images is a simple means of determining the pH value since these data correlate well with the data obtained by the spectrophotometer. In the later stages of the study, improving the system's sensitivity will be investigated to improve the performance.

REFERENCES

1. Promphet, N., Rattanawaleedirojn, P., Siralertmukul, K., Soatthiyanon, N., Potiyaraj, P., Thanawattano, C., Hinestroza, J.P., Rodthongkum, N., (2019), *Non-invasive textile based colorimetric sensor for the simultaneous detection of sweat pH and lactate*, Talanta, 192, 424-430.
2. Pávai, M., Orosz, E. & Paszternák, A., (2016), *Smartphone-Based Extension of the Curcumin/Cellophane pH Sensing Method*, Food Analytical Methods, 9, 1046-1052.
3. De Clerck, K., Geltmeyer, J., Steyaert, I., & Van der Schueren, L. (2012), *Halochromic textile materials as innovative pH-sensors*, Advances in Science and Technology, 80, 47-52.
4. Choi, M-Y., Lee, M., Kim, J-H., Kim, S., Choi, J., So, J-H., Koo, H-J., (2022), *A fully textile-based skin pH sensor*, Journal of Industrial Textiles, 51, 1, 441S-457S.
5. Hewlings, S.J., Kalman, D.S., (2017), *Curcumin: A Review of Its Effects on Human Health*, Foods, 6, 10, 92.
6. Pourreza, N., & Golmohammadi, H., (2015), *Application of curcumin nanoparticles in a lab-on-paper device as a simple and green pH probe*, Talanta, 131, 136-141.
7. Zhao, Q., Kong, D-X., Zhang, H-Y., (2008), *Excited-state pKa values of Curcumin*, Natural Product communications, 3, 2, 229-332.
8. Kharat, M., Du, Z., Zhang, G., McClements, DJ., (2017), *Physical and Chemical Stability of Curcumin in Aqueous Solutions and Emulsions: Impact of pH, Temperature, and Molecular Environment*, Journal of Agricultural and Food Chemistry, 65, 8, 1525-1532.
9. Salaün, F., Bedek, G., Devaux, E., Dupont, D., (2011), *Influence of the washings on the thermal properties of polyurea-urethane microcapsules containing xylitol to provide a cooling effect*, Materials Letters, 65, 2, 381-384.
10. Souguir, H., Salaün, F., Douillet, P., Vroman, I., Chatterjee, S., (2013), *Nanoencapsulation of curcumin in polyurethane and polyurea shells by an emulsion diffusion method*, Chemical Engineering Journal, 221, 133-145.
11. Salaün, F., Bedek, G., Devaux, E., Dupont, D., Gengembre, L., (2011), *Microencapsulation of a cooling agent by interfacial polymerization: influence of the parameters of encapsulation on poly(urethane-urea) microparticles characteristics*, Journal of Membrane Science, 370, 1-2, 23-33.
12. Salaün, F., Vroman, I., (2009), *Curcumin-loaded nanocapsules: formulation and influence of the nanoencapsulation processes variables on the physico-chemical characteristics of the particles*, International Journal of chemical Reactor Engineering, 7, A55.